

Article

Complete Evaporation of Black Holes and Page Curves

Irina Aref'eva  and Igor Volovich *

Steklov Mathematical Institute, Russian Academy of Sciences, Gubkina Str. 8, 119991 Moscow, Russia

* Correspondence: volovich@mi-ras.ru

Abstract: The problem of complete evaporation of a Schwarzschild black hole, the simplest spherically symmetric vacuum solution of the Einstein field equation, posed by Hawking, is that when the black hole mass M disappears, an explosion of temperature $T = 1/8\pi M$ takes place. We consider the Reissner–Nordstrom black hole, a static spherically symmetric solution to the Einstein–Maxwell field equations, and show that if mass M and charge $Q < M$ satisfy the bound $Q > M - CM^3$, $C > 0$ for small M , then the complete evaporation of black holes without blow-up of temperature is possible. We describe curves on the surface of state equations such that the motion along them provides complete evaporation without temperature explosion. In this case, the radiation entropy follows the Page curve and vanishes at the end of evaporation. Similar results for rotating Kerr, Schwarzschild–de Sitter and Reissner–Nordstrom–(Anti)-de Sitter black holes are discussed.

Keywords: black holes; near extremal black holes; Hawking radiation; black hole evaporation; black information problem

1. Introduction

It was suggested by Hawking that the Schwarzschild black holes, simplest spherically symmetric vacuum solution of the Einstein field equations, produce radiation like black bodies with temperature of $T = 1/8\pi M$, where M is the mass of the black hole [1]. This formula is derived for a fixed Schwarzschild background metric, where the mass could be arbitrary small. Note that, temperature becomes infinite for vanishing mass. It is a question whether to consider this formula till $M = 0$ or deal only with mass more than the Planck mass. This question is closely related with the question whether is it possible to consider complete black hole evaporation or one has to stop when the mass is close to the Planck mass [1–5]. Here we do not discuss the process of evaporation of a dynamical black hole with its well-known back reaction problems and quantum gravitational corrections on Planck scales, however, for simplicity, we refer to the limit $M \rightarrow 0$ as the complete evaporation of a black hole. In this paper, we study under which conditions in classical gravity the limit of a vanishing black hole mass is possible without $T \rightarrow \infty$.

According to the Stefan–Boltzmann law, the energy density E of black body radiation with temperature T is given by $E = \pi^2 T^4/15$. Therefore from Hawking's formula for the temperature, it follows that the energy density of the radiation, emitted by a black hole behaves at small M as M^{-4} . If the mass of the black hole disappears during evaporation, then the black hole releases an infinite amount of energy, which is clearly unphysical. Hawking drew attention to this problem in his first paper on the evaporation of black holes with the title “Black hole explosions?” [6].

The information loss problem [2,7] is closely related to this unphysical behaviour, since the radiation entropy S_R diverges for small M as M^{-3} . One can say that because of this infinity, complete evaporation never occurs in nature, and we cannot obtain complete evaporation, which ends only by thermal radiation being obviously a mixed state. Just the evolution of the initially pure quantum state to this mixed state breaks unitarity and leads to information paradox.



Citation: Aref'eva, I.; Volovich, I. Complete Evaporation of Black Holes and Page Curves. *Symmetry* **2023**, *15*, 170. <https://doi.org/10.3390/sym15010170>

Academic Editor: Kazuharu Bamba

Received: 16 November 2022

Revised: 28 December 2022

Accepted: 3 January 2023

Published: 6 January 2023



Copyright: © 2023 by the authors. Licensee MDPI, Basel, Switzerland. This article is an open access article distributed under the terms and conditions of the Creative Commons Attribution (CC BY) license (<https://creativecommons.org/licenses/by/4.0/>).

In this paper, a possible mechanism for the complete evaporation without temperature explosion of black holes in the framework of classical gravity is discussed. This mechanism also ensures that the entropy of radiation vanishes in the limit when the mass of the black hole tends to zero, which is consistent with unitary evolution. We note that the complete evaporation without explosion of temperature and energy is possible if the black hole possess addition parameters—a charge Q or an angular momentum a , or we deal with non-zero cosmological constant and we are in near-extremal regimes.

In the case of the Reissner–Nordstrom black hole, a static spherically symmetric solution to the Einstein–Maxwell field equations, if the mass M and charge $Q < M$ satisfy also the bound

$$Q > M - CM^3, \quad C > 0, \tag{1}$$

for small mass M , then the Hawking temperature for the charged black hole

$$T = \frac{1}{2\pi} \frac{\sqrt{M^2 - Q^2}}{(M + \sqrt{M^2 - Q^2})^2} \tag{2}$$

tends to 0 when $M \rightarrow 0$.

We can describe special curves in the domain (1). The expression (2) defines the surface Σ of the state equation $T = T(M, Q)$ in the three-dimensional space with coordinates (M, Q, T) . The evaporation process is described by a curve σ on Σ , see Figure 1A in Section 2. It is convenient to make the change of variables $(M, Q) \rightarrow (M, \lambda)$, $\lambda = \sqrt{M^2 - Q^2}$. We describe an evaporation curve σ by a function $\lambda = \lambda(M)$ and the charge belong to this curve is

$$Q^2 = M^2 - \lambda(M)^2, \tag{3}$$

where $0 < \lambda(M) < M$. Obviously, the Reissner–Nordstrom solution of the Einstein equations with parameters M and Q will still be a solution if the charge Q is taken to depend on the mass M . The Hawking temperature T becomes

$$T = \frac{\lambda(M)}{2\pi(M + \lambda(M))^2}. \tag{4}$$

If we take $\lambda(M)$ such that for small M it obeys $\lambda(M) = o(M^2)$, then T tends to 0 as $M \rightarrow 0$ and we get the complete evaporation of the black hole. Therefore, for small M , the evaporating black hole must be in a state close to the extreme one.

In this paper we consider two particular examples of near-extremal Reissner–Nordstrom black holes.

- We take

$$\lambda(M) = CM^\gamma, \quad C > 0, \quad \gamma > 2. \tag{5}$$

This means that for small M we are dealing with almost extreme regime. An interesting case is when $\gamma = 2$, i.e., $\lambda(M) = CM^2$. In this case, the limit of temperature when $M \rightarrow 0$ is not equal to zero, but is equal to $C/2\pi$, although the mass and charge are vanishing. In the cases with $\gamma \geq 2$ the mass dependence of charge has a deformed bell-shaped form (see Figure 2A below).

- We also consider the case then the function $T = T(M)$ is given. In this case one can solve the quadratic Equation (4) and find the function $\lambda(M)$. We take as an example the temperature of the form

$$T(M) = C\sqrt{M(M_0 - M)}, \tag{6}$$

where C and M_0 are positive constants and $0 \leq M \leq M_0$. The radiation entropy $S_{rad}(M)$ is proportional to T^3 so in this case one has $S_R(M_0) = S_R(0) = 0$.

Note that we do not discuss here under what physical conditions Equations (5) or (6) can be realised.

As mentioned above, the problem of temperature explosion during evaporation of the black hole is closely related with the information paradox. In the context of studying the information paradox, Page [3,7] suggested that the Schwarzschild black holes evaporate completely, and the radiation entropy of evaporating black holes first increases, but then decreases and tends to zero when the black hole mass vanishes. This hypothetical behaviour is known as the Page curve. Recent works devoted to the information paradox are aimed to obtain the Page curve [8–10] for the entanglement entropy of radiation. In this work we deal with the usual thermodynamic entropy for radiation that is proportional to T^3 . So if temperature decreases with vanishing of mass then the entropy of radiation decreases too. To get the time dependence of this evolution we consider charge and mass change during the black hole evaporation.

The loss of the mass and charge during evaporation of the Reissner–Nordstrom black hole is a subject of numerous considerations. Changes in mass and charge during the evaporation of a RN black hole satisfy a system of two coupled equations (see below Equations (28) and (29)). Assuming that the relation between mass and charge is fixed, we are left with a single non-linear differential equation

$$\frac{dM}{dt} = -f(M), \quad (7)$$

where an explicit expression for the function $f(M)$ is given in Section 2.3. For small M and $\lambda(M) = CM^\gamma$, $\gamma > 2$ we get mass evolution in the form

$$M(t) = \frac{M_0}{(1+Bt)^{1/(3\gamma-6)}}, \quad t \geq 0, \quad (8)$$

where M_0 and B are positive constants. This form of time dependence of the mass of an evaporating black hole, together with the dependence of the entropy of radiation as T^3 , gives the Page form of the evolution of the entropy of radiation over time, see Section 2.3. If $\gamma = 2$ then $M(t) = M_0 e^{-Bt}$. In this case, the lifetime of a black hole is infinite.

For Kerr (axially symmetric rotating black hole), Schwarzschild-de Sitter (spherically symmetric solution to the Einstein field equation with positive cosmological constant) and Reissner–Nordstrom-(Anti)-de Sitter (spherically symmetric solution to the Einstein–Maxwell field equations with (negative) positive cosmological constant) black holes, we also indicate the curves on the equation of the state surfaces along which the complete evaporation of black holes occurs without thermal explosions.

The paper is organised as follows. In Section 2 models of complete evaporation of the Reissner–Nordstrom black hole accompanied by the temperature goes to 0 are considered. In Section 3 the models of complete evaporation of the Kerr black hole are investigated and in Section 4 these results are generalised to the Kerr–Newman black hole. Complete evaporation of the Schwarzschild–de Sitter black hole is considered in Section 5. In Section 6 we discuss complete evaporation of Reissner–Nordstrom-(Anti)-de Sitter black holes. Section 7 contains summary and discussions.

2. Complete Evaporation of the Reissner–Nordstrom Black Hole

We consider a model of complete evaporation of a Reissner–Nordstrom (RN) black hole with the following metric

$$ds^2 = -f(r)dt^2 + f(r)^{-1}dr^2 + r^2d\Omega^2, \quad (9)$$

where

$$f(r) = 1 - \frac{2M}{r} + \frac{Q^2}{r^2}, \quad (10)$$

here M and Q are mass and charge of the black hole. It is assumed that $M^2 \geq Q^2$. The blackening function (10) can be presented as

$$f = (r - r_+)(r - r_-)/r^2, \tag{11}$$

where

$$r_{\pm} = M \pm \sqrt{M^2 - Q^2}. \tag{12}$$

The temperature of the Reissner–Nordstrom black hole is

$$T = \frac{1}{2\pi} \frac{\sqrt{M^2 - Q^2}}{(M + \sqrt{M^2 - Q^2})^2} \tag{13}$$

2.1. Evaporation Curves and Bell-Shaped Temperature

We take Q to be a function on M of the form (3). The Hawking temperature T under this constraint becomes equal to

$$T = \frac{\lambda(M)}{2\pi(M + \lambda(M))^2}. \tag{14}$$

Depending on the behaviour of the function $\lambda(M)$ we have:

- if $\lambda(M)$ satisfies for small M the bounds

$$0 < \lambda(M) \leq CM^\gamma, \quad C > 0, \gamma > 2 \tag{15}$$

then $T \rightarrow 0$ as $M \rightarrow 0$ and one gets the complete evaporation of black hole;

- if the function $\lambda(M)$ satisfies the bounds

$$0 < \lambda(M) \leq C \frac{M^\gamma}{A + M^{\gamma+1}}, \quad C > 0, A > 0, \gamma > 2 \tag{16}$$

then the temperature $T \rightarrow 0$ also for $M \rightarrow \infty$;

- if the function $\lambda(M)$ is

$$\lambda(M) = \frac{M^\gamma}{A + M^{\gamma-1}}, \quad A > 0, \gamma > 3, \tag{17}$$

then the temperature $T \rightarrow 0$ and $Q \rightarrow 0$ also for $M \rightarrow \infty$. Note that the asymptotic of T at $M \rightarrow \infty$ coincides with the Schwarzschild case.

The entropy and the free energy under constraint (3) are equal

$$S_{RN} = \pi r_+^2 = \pi(M + \lambda(M))^2 \tag{18}$$

$$G_{RN} = M - TS = M - \frac{1}{2}\lambda(M) \tag{19}$$

Note that the entropy S_{RN} and the free energy G_{RN} go to 0 as $M \rightarrow 0$ for λ satisfying (15).

Let us suppose that the temperature is given by a function $T = T(M)$. We solve the quadratic Equation (14) and find two functions

$$\lambda_{\pm}(M) = \frac{1 - 4\pi MT \pm \sqrt{1 - 8\pi MT}}{4\pi T} \tag{20}$$

Both solutions are real for

$$1 - 8\pi MT(M) \geq 0. \tag{21}$$

2.2. Examples

2.2.1. Deformed Bell-Shaped Dependence of Charge on Mass M

Equation (13) defines the surface Σ of the state equation for Reissner–Nordstrom black hole. This surface is shown in Figure 1A. The same surface is shown in Figure 1B in (M, λ, T) coordinates, Equation (14).

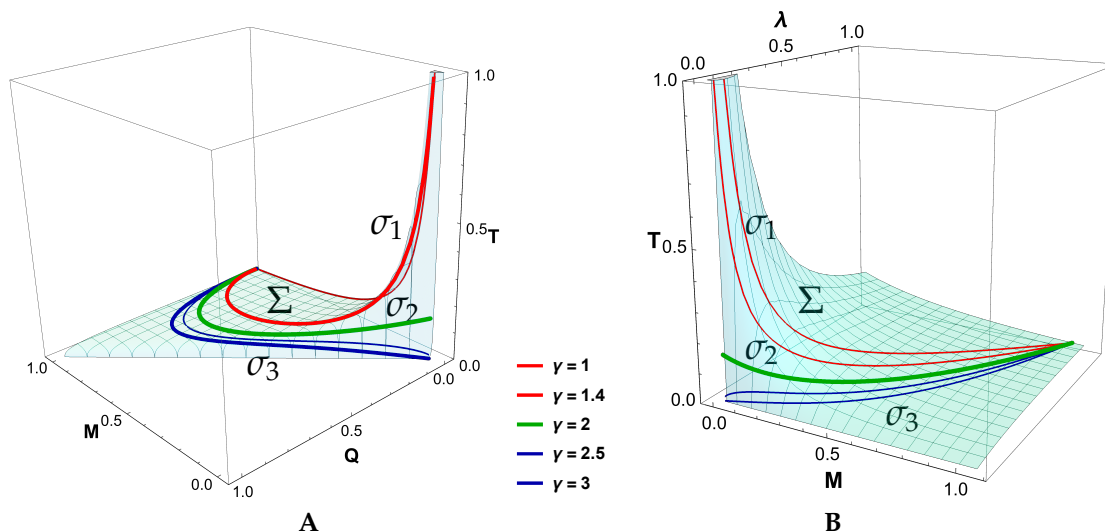


Figure 1. (A) The 3D plot shows the dependencies of the temperature on the mass M and the charge Q . 3D curves σ_γ show the dependence of the temperature on the mass along the constrains (3) with $\lambda(M) = M^\gamma$, $\gamma = 1, 1.4, 2, 2.5, 3$. (B) The 3D plot shows the dependencies of the temperature on the mass M and λ . 3D curves σ_γ show the dependence of the temperature on the mass along the constrain (3) with $\lambda(M) = M^\gamma$, $\gamma = 1, 1.4, 2, 2.5, 3$.

The 3D curves in Figure 1A,B show the dependence of temperature on mass along the curves

$$\lambda(M) = \left(\frac{M}{m_0}\right)^\gamma. \tag{22}$$

with different $\gamma = 1, 1.4, 2, 2.5, 3$. We see that on some curves the temperature tends to infinity as $M \rightarrow 0$ (for these curves $\gamma < 2$), while on curves with $\gamma > 2$ the temperature tends to zero as $M \rightarrow 0$.

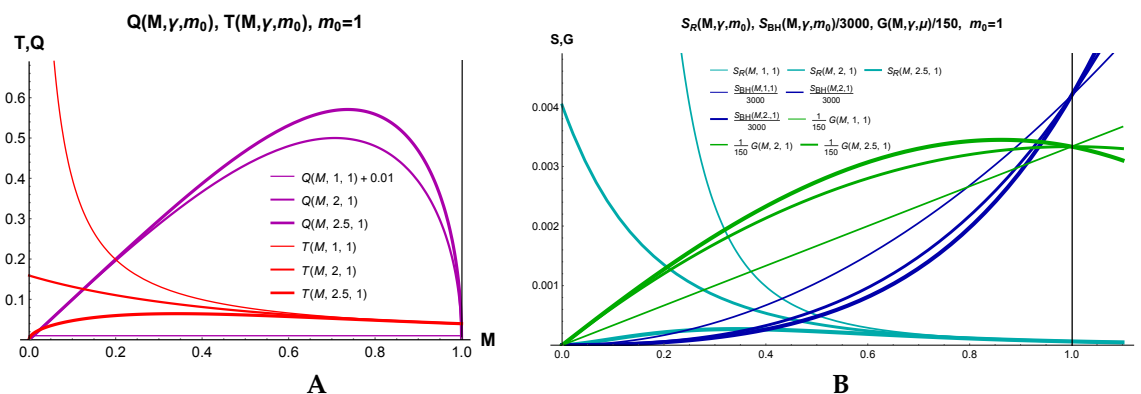


Figure 2. (A) The graph shows charge Q (magenta) and temperature T (red) versus M for different values of the scaling parameter γ , $\gamma = 1, 2, 2.5$. (B) The graph shows dependencies of free energy G (green), black hole entropy S (blue) and radiation entropy (dark cyan) on M for scale parameter $\gamma = 1, 2, 2.5$. The black lines show the boundaries of the allowed regions for M .

Mass dependence of charge Q , temperature T , entropy and free energy at (22) with different γ parameters and the same $\mu = 1$ parameter are shown in Figure 2. We see that for

all $\gamma > 1$ there is a restriction on M , $M \leq 1$. The temperature and entropy of the radiation tend to zero at $M \rightarrow 0$ for $\gamma > 2$, to a nonzero constant for $\gamma = 2$, and to infinity for $\gamma < 2$. In this case, the temperature and radiation entropy S_R at $\gamma > 2$, starting from the initial value at $M = 1$, increase to a certain maximum value, then decrease to zero, i.e., the mass dependencies T and S_R have deformed bell shapes (the thickest red and dark cyan lines in Figure 2A,B, respectively). In the case of a slow dependence of mass on time during black hole evaporation, the dependence of radiation entropy on mass, represented in Figure 2B by the dark cyan line, leads to the Page form of the time evolution of radiation entropy, see Section 2.3. The entropy of a black hole and the free energy tend to zero at $M \rightarrow 0$ for all values of γ . We also see, Figure 2A, that the shape of Q versus M is a deformed bell (except in the case of $\gamma = 1$ and $Q = 0$, which corresponds to the Schwarzschild case). Note that in Figure 2B one can see that the free energy increases as the black hole mass decreases. This corresponds to the region M , where the charge increases with decreasing mass M .

In our recent paper [11] we found restrictions on γ in (22) under which the entanglement entropy calculated with the island formula has no explosion at $M \rightarrow 0$.

2.2.2. Semi-Circle Dependence of Temperature on Mass M

One can take the semi-circle form of T dependence on M (6) with $C = 1$. The condition (21) gives a restriction on possible values on admissible M_0 . Indeed, substituting (6) to the condition (21) we get

$$1 - 8\pi M\sqrt{M(M_0 - M)} \geq 0, \tag{23}$$

that should be satisfied for all $M < M_0$. This can be realised for $M_0 \leq M_{0,cr} = 2^{1/2}/\pi^{1/2}3^{3/4} \approx 0.35$.

We plot in Figure 3A λ as a function of M for two branches $\lambda_{\pm} = \lambda_{\pm}(M)$ given by (20), where T is defined by (6). We see that for small $M_0 \lesssim 0.35$ both λ_{\pm} are real. For $M_0 \gtrsim 0.35$ two solutions λ_{\pm} are real only on parts of the interval $[0, M_0]$ (dashed blue lines in Figure 3A). For small M and $M_0 \lesssim 0.35$ we have

$$\lambda_{-}(M, M_0) = 2\pi M^{5/2}\sqrt{M_0} + \mathcal{O}(M^{7/2}), \tag{24}$$

$$\lambda_{+}(M, M_0) = \frac{1}{2\pi\sqrt{M}\sqrt{M_0}} + \mathcal{O}(M^{1/2}), \tag{25}$$

and in accordance with (21) we consider only the λ_{-} -branch.

We plot in Figure 3B the mass dependence of the charge Q , that is defined by (3) with $\lambda = \lambda_{-}(M)$.

We have the following asymptotic behaviour of $T(M, M_0)$, $S_{BH}(M, M_0)$, $G(M, M_0)$ and $S_R(M, M_0)$ for small M

$$T(M, M_0) = \sqrt{M}\sqrt{M_0} + \mathcal{O}(M^{1/2}), \quad S_{BH}(M, M_0) = \pi M^2 + \mathcal{O}(M^{7/2}) \tag{26}$$

$$G(M, M_0) = M + \mathcal{O}(M^{5/2}), \quad S_R(M, M_0) = M^{3/2}M_0^{3/2} + \mathcal{O}(M^{5/2}). \tag{27}$$

The plot in Figure 4A shows the dependences of the temperature and the entropy of radiation on $M \leq M_0$ for two different M_0 , $M_0 < M_{0,cr}$ and $M_0 = M_{0,cr} \approx 0.35$. As has been noted above, there is no real solution for $M_0 > M_{0,cr}$. The plot in Figure 4B shows dependences of the entropy (blue) and free energy (green) of the Reissner–Nordstrom black hole on M calculated on the branch λ_{-} for different $M_0 \leq M_{0,cr}$. The vertical black lines indicate the value of M_0 , $M \leq M_0$. It is interesting to note that both entropies, the black hole entropy and the radiation entropy, have the form suitable to realize the Page curves—they first increase from some initial values, in particular from zero values for the case of the radiation entropy, up to some maximal value, then start to decrease to zero at $M \rightarrow 0$.

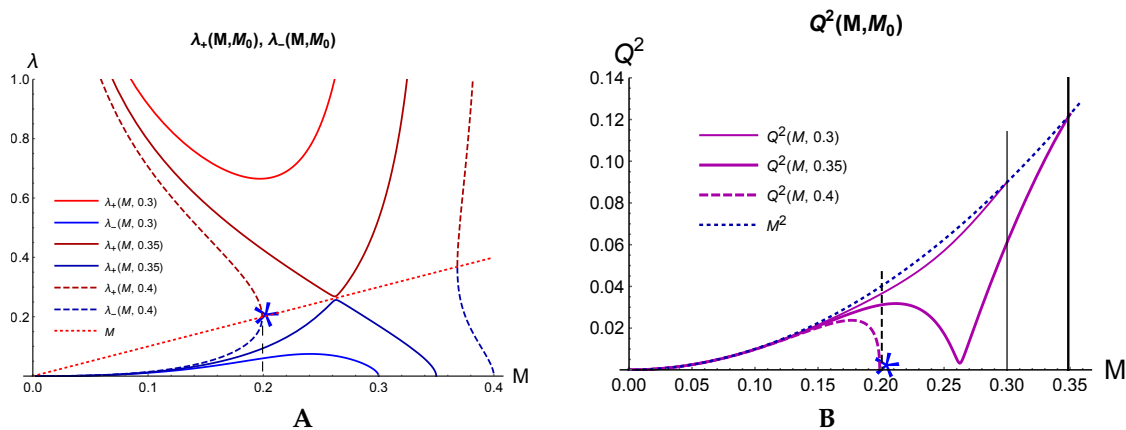


Figure 3. (A) λ as a function of M for two branches $\lambda_{\pm} = \lambda_{\pm}(M)$ given by (20), where T is defined by (6). The dashed red line corresponds to $\lambda = M$ and we see that the λ_+ is not a physical solution, since $\lambda_+ > M$. We also see that real solutions exist for all $M \leq M_0$ if $M_0 < M_{0,cr} \approx 0.35$ (blue solid lines) and for $M < M_{cr}(M_0)$ for $M_0 > M_{0,cr}$ (dashed blue line). We do not consider the right part of λ_- , since it does not admit the $M \rightarrow 0$ limit. (B) Q^2 vs M for $\lambda_-(M)$ as in (A). Solid magenta lines correspond to $M_0 < M_{0,cr}$ and the dashed magenta line to $M_0 > M_{0,cr}$. The points indicated by * correspond to the Schwarzschild case.

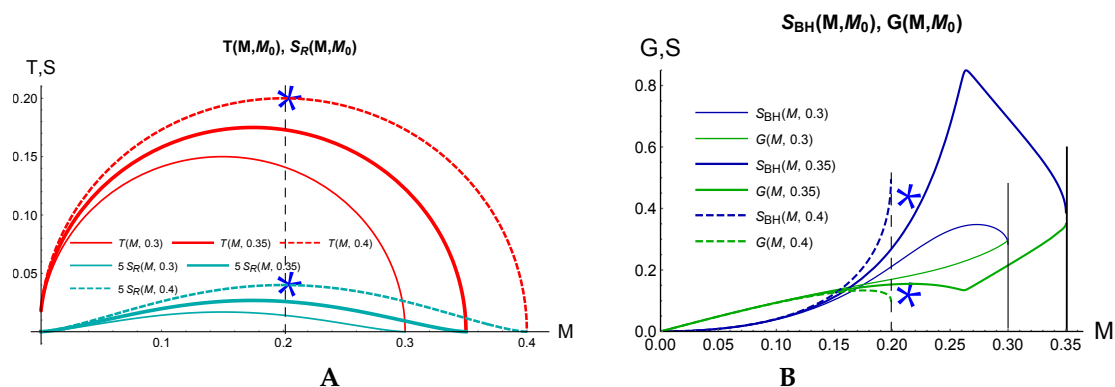


Figure 4. (A) The plot shows mass dependences of the temperature (red) and the entropy of radiation (cyan) for three different M_0 : $M_0 = 0.3, M_0 = 0.35$ and $M_0 = 0.4$. In the first two cases (solid lines) $M \leq M_0$, and in the third one (dashed line) $M < M_{cr}(M_0), M_0 > M_{0,cr} = 0.3501$. (B) The plot shows mass dependences of the entropy (blue) and free energy (green) of the Reissner–Nordstrom black hole for the same M_0 as in (A). The vertical solid black lines indicate the value of M_0 and $M \leq M_0$ and the dashed vertical line shows $M_{cr}(0.4)$.

2.3. Time Evolution

The loss of the mass and charge during evaporation of RN black hole is a subject of numerous consideration [12–20] and references therein.

In the case of fixed relations (3), we consider the following system of equations

$$\frac{dM}{dt} = -A\sigma T^4 + \frac{Q}{r_+} \frac{dQ}{dt}, \tag{28}$$

$$\frac{dQ}{dt} = \frac{M - \lambda \lambda'}{\sqrt{M^2 - \lambda^2}} \frac{dM}{dt}, \tag{29}$$

where A is a positive constant and the cross-section σ is proportional to M^2 for small M . The first equation in the system of Equations (28) and (29) coincides with the equation

considered in [17], and the second is obtained by simply differentiating the relation (3). From (28) and (29) we get

$$\frac{dM}{dt} = -\frac{A\sigma T^4(M + \lambda)}{\lambda(1 + \lambda')} \tag{30}$$

For $\lambda(M) = CM^\gamma$ and small M one gets

$$\frac{dM}{dt} = -C_1 M^{3\gamma-5} \tag{31}$$

This equation for $\gamma > 2$ and $M(0) = M_0$ has a solution

$$M(t) = \frac{M_0}{(1 + Bt)^{\frac{1}{3(\gamma-2)}}, \quad B = \frac{3(\gamma-2)C_1}{M_0^{6-3\gamma}}, \quad \gamma > 2, \tag{32}$$

where M_0 and B are positive constants. For $\gamma = 2$ we have

$$M(t) = M_0 e^{-C_1 t} \tag{33}$$

One obtains an infinitely large time of the complete evaporation of charged black hole under constraint (3).

In Figure 5 we present two different regimes of mass versus time, Figure 5A,D, the former with a finite decay time and the latter with an infinite decay time. Because of the dependence of radiation entropy on mass shown in Figure 5B, these two different types of time dependence on mass result in two different entropy versus time dependences, Figure 5C,E. However, these two graphs do not differ significantly if we consider them on the interval $(0, t_1)$, here $t_{Page} < t_1$. In both cases, entropy first increases with time, then decreases after Page time t_{Page} . Note that if $M_m > M_1 > M_{Plack}$, we can ignore the effects of quantum gravity in the above consideration.

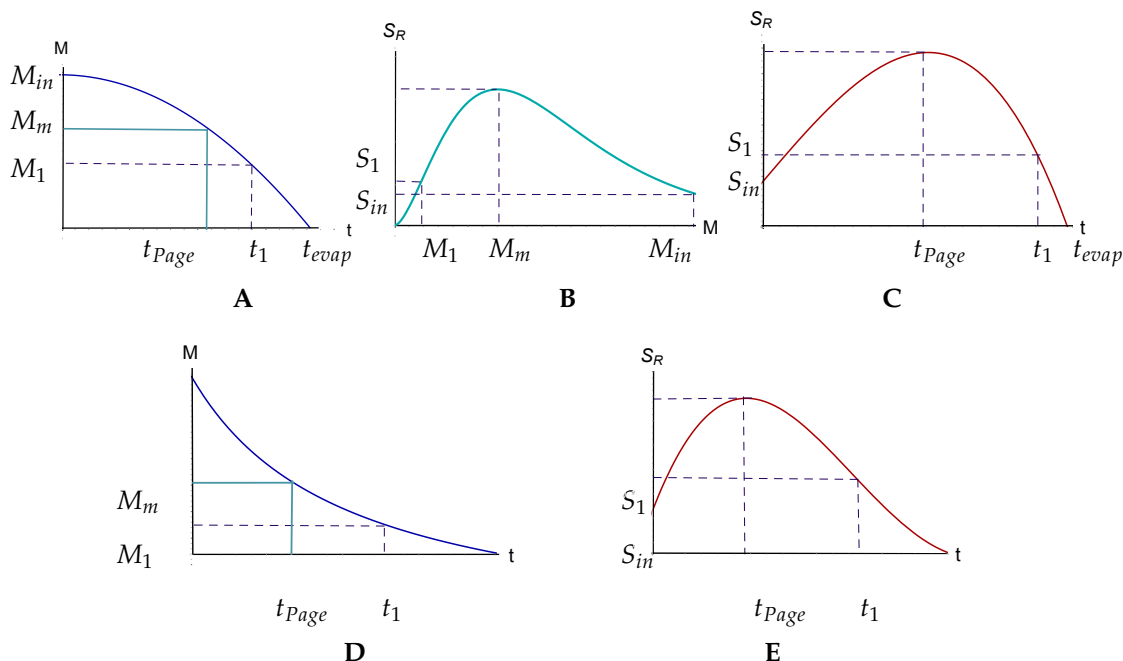


Figure 5. Page curves for radiation entropy and mass dependencies of the radiation entropy. (A) Time dependence of the mass of a black hole that evaporates in a finite time. (B) Dependence of the radiation entropy of on the mass of a black hole. (C) Time dependence of the radiation entropy of a black hole evaporating in a finite time. (D) Time dependence of the black hole mass, which evaporates infinitely. (E) Time dependence of the radiation entropy of a black hole which evaporates indefinitely.

3. Complete Evaporation of the Kerr Black Hole

The Kerr metric in Boyer–Lindquist coordinates reads

$$ds^2 = -\frac{\Delta - a^2 \sin^2 \theta}{\Sigma} dt^2 - 2a \sin^2 \theta \frac{r^2 + a^2 - \Delta}{\Sigma} dt d\phi + \frac{(r^2 + a^2)^2 - \Delta a^2 \sin^2 \theta}{\Sigma} \sin^2 \theta d\phi^2 + \frac{\Sigma}{\Delta} dr^2 + \Sigma d\theta^2 \quad (34)$$

where

$$\begin{aligned} \Sigma &= r^2 + a^2 \cos^2 \theta, \\ \Delta &= r^2 - 2Mr + a^2 = (r - r_+)(r - r_-). \end{aligned} \quad (35)$$

The outer and inner horizon are located at $r = r_+, r_-$ respectively and

$$r_{\pm} = M \pm \sqrt{M^2 - a^2} \quad (36)$$

The temperature of the Kerr black hole is

$$T_{Kerr} = \frac{1}{4\pi} \frac{\sqrt{M^2 - a^2}}{M(M + \sqrt{M^2 - a^2})} \quad (37)$$

When M equal to a one gets an extremal black hole with $T = 0$.

If the angular momentum $a < M$ also satisfies the bound

$$a > M - CM^3, \quad C > 0, \quad (38)$$

for small mass M , then the Hawking temperature T_{Kerr} tends to 0 when $M \rightarrow 0$.

If we take a to be a function of M of the form

$$a^2 = M^2 - \lambda(M)^2, \quad (39)$$

where the function $0 < \lambda(M) \leq M$, then the temperature T becomes equal to

$$T_{Kerr} = \frac{\lambda(M)}{4\pi M(M + \lambda(M))}, \quad (40)$$

and the entropy and the free energy are

$$S_{Kerr} = \pi r_+^2 = \pi(M + \lambda(M))^2, \quad (41)$$

$$G_{Kerr} = M - T_{Kerr} S_{Kerr} = M - \frac{\lambda(M)(M + \lambda(M))}{4M}. \quad (42)$$

If $\lambda(M) = o(M^2)$ as $M \rightarrow 0$, then $T_{Kerr} \rightarrow 0$.

Similar to the RN case, if one takes the function $\lambda(M)$ as

$$\lambda(M) = \frac{M^\gamma}{A + M^{\gamma-1}}, \quad A > 0, \gamma > 3, \quad (43)$$

then the temperature $T \rightarrow 0$ and $a \rightarrow 0$ also for $M \rightarrow \infty$.

3.1. Examples

3.1.1. Deformed Bell-Shaped Evaporation Curves

As in the previous Section 2, we first consider the case (22). The behaviour of the charge a , the temperature T , the entropy and the free energy as functions of M for the

curves (39) with different scaling parameter γ and the same parameter $\mu = 1$ are presented in Figure 6. These plots are very similar to the plots presented in Figure 2 for the RN case. For all $\gamma > 1$ there is a restriction on M , $M \leq 1$ and the temperature and the radiation entropy go to zero as $M \rightarrow 0$ for $\gamma > 2$, to a non-zero constant for $\gamma = 2$ and to the infinity for $\gamma < 2$. Moreover, the radiation entropy at $\gamma > 2$, starting from the initial value at $M = 1$, first increases to a certain maximum value, then decreases to zero, i.e., has a form that, in the case of a slow decrease in mass during evaporation, provides the form of the Page dependence of the radiation entropy on time, see Figure 5. The black hole entropy (blue lines, Figure 2B) and the free energy (green lines, Figure 2B) go to zero when $M \rightarrow 0$ for $\gamma \geq 1$. We also see, Figure 6A, that the form of dependence of a on M is a deformed bell, compare with Figure 2A.

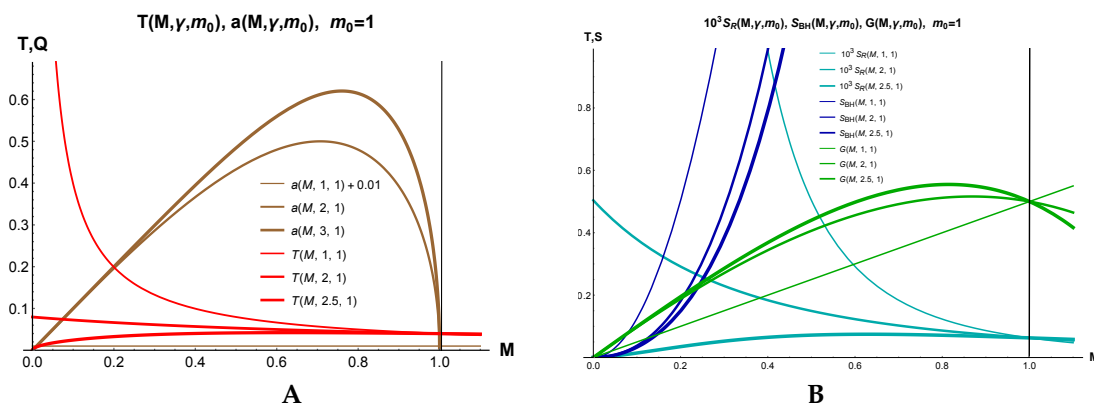


Figure 6. The plot shows the dependence of the temperature T (red), the angular momentum a (brown), the free energy G (green), the black hole entropy S (blue) and the radiation entropy (cyan) for the curves (39) with function λ given by (22) with different scaling parameter $\gamma = 1, 2, 2.5, 3$ and $\mu = 1$.

3.1.2. Semi-Circle Dependence of Temperature on Mass M

If the function $T(M)$ is given, then from Equation (40) we obtain

$$\lambda(M) = \frac{4\pi M^2 T(M)}{1 - 4\pi M T(M)}. \tag{44}$$

Unlike (14), now the equation relating T and λ , i.e., Equation (40), is linear on λ which gives us (44). Assuming the temperature dependence on M is the same as for the RN case, (6), we get

$$\lambda(M, M_0) = \frac{4\pi M^2 \sqrt{M(M_0 - M)}}{1 - 4\pi M \sqrt{M(M_0 - M)}}. \tag{45}$$

Note that the explicit forms of $\lambda(M)$ in the RN and Kerr cases are different, compare (20) with (44).

For small M_0 from (45) follows that $\lambda(M, M_0) < M$ and the constraint (39) corresponds to positive values of a^2 . At the critical value of $M_{0,cr}$ the following equation

$$M^2 - \frac{16\pi^2 M^5 (M_0 - M)}{(1 - 4\pi M \sqrt{M(M_0 - M)})^2} = 0, \tag{46}$$

has one real solution, $M_{0,cr} \approx 0.35003$, and $M_1 \approx 0.261$. For $M_0 > M_{0,cr}$ Equation (46) has two real solutions, for example, for $M_0 = 0.4$ shown in Figure 7, there are two real solutions $M_1 = 0.199$, $M_2 = 0.368$. Indeed, in the plots in Figure 7A we see that $\lambda(M, M_0) < M$ for $M_0 < 0,35$ and for $M_0 > 0,4$ there are two intersections of the gray dashed line represented $\lambda(M, M_0)$ with the red dotted line. The case of one real root of Equation (46) is shown by thick blue line in Figure 7A and thick blue line in Figure 7B.

The plots in Figure 7C show mass dependences of the temperature $T(M, M_0)$ and the entropy of radiation, $S(M, M_0)$ and the plot in Figure 7D show mass dependences of the black hole entropy and the free energy on M for different M_0 .

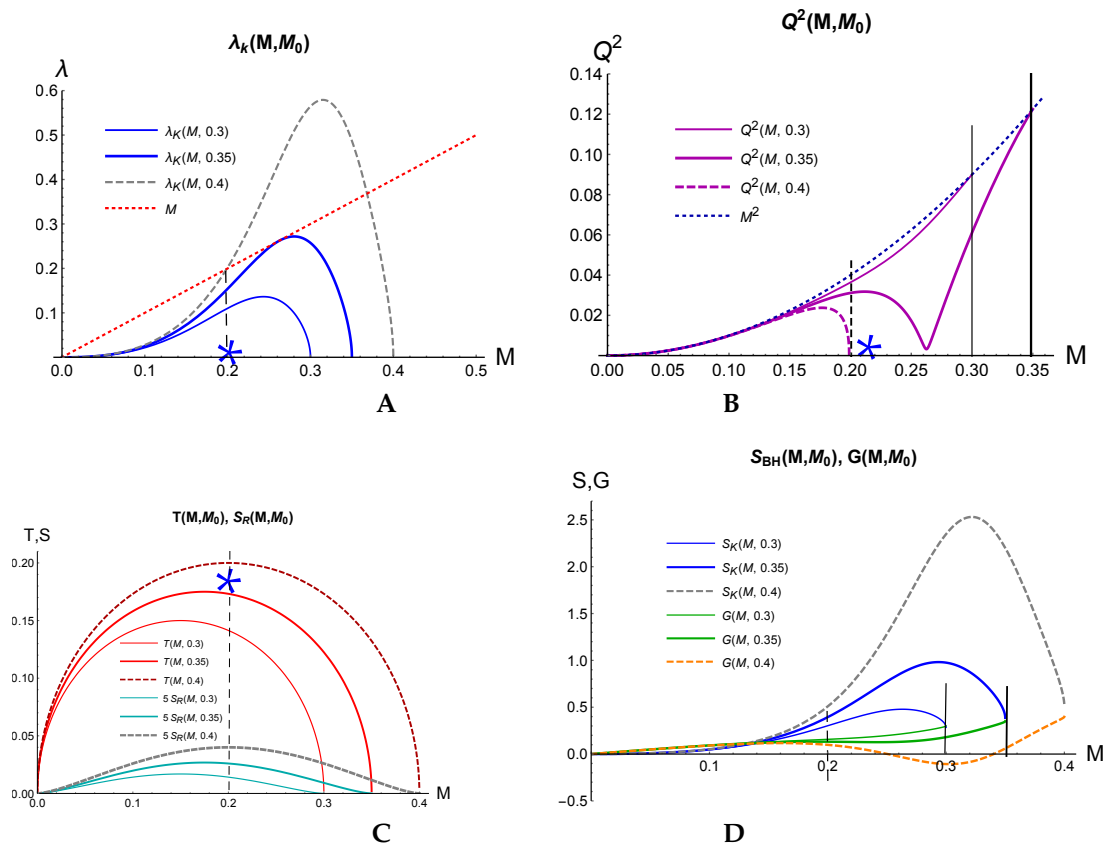


Figure 7. (A) The plots show the dependence of λ on M given by (45) for $M_0 = 0.3, 0.35, 0.4$. (B) The plots show curves corresponding to the curves presented in (A). Plots in (C) show the mass dependences of the temperature and the radiation entropy for the curves presented in (B), and the mass dependences of the free energy and the black hole entropy for these curves are presented in (D).

4. Complete Evaporation of the Kerr–Newman Black Hole

The Kerr–Newman (KN) metric is

$$\begin{aligned}
 ds^2 = & -\frac{1}{\rho^2}(\Delta_r - a^2 \sin^2 \theta)dt^2 + \frac{\rho^2}{\Delta_r}dr^2 + \rho^2 d\theta^2 \\
 & + \frac{1}{\rho^2}[(r^2 + a^2) - \Delta_r a^2 \sin^2 \theta] \sin^2 \theta d\varphi^2 - \frac{2a}{\rho^2}[(r^2 + a^2) - \Delta_r] \sin^2 \theta dt d\varphi,
 \end{aligned}
 \tag{47}$$

where $\rho^2 = r^2 + a^2 \cos^2 \theta$, $\Delta_r = (r^2 + a^2) - 2Mr + q^2$. Here the parameters M, a and q are the mass, the angular momentum, and the charge of the black hole, respectively. The electromagnetic potential is

$$A_\mu = -\frac{qr}{\rho^2}(1, 0, 0, -a \sin^2 \theta).
 \tag{48}$$

There are two horizons r_\pm and

$$r_+ = M + \sqrt{M^2 - (a^2 + q^2)}.
 \tag{49}$$

The Hawking temperature of the black hole horizon is given by

$$T_{KN} = \frac{r_+ - M}{2\pi(r_+^2 + a^2)}. \tag{50}$$

We can put the constraint

$$a^2 + q^2 = M^2 - \lambda^2(M), \tag{51}$$

where $\lambda(M)$ is a function of M . Substituting (51) into (50) we get

$$T_{KN} = \frac{\lambda(M)}{2\pi(2M^2 + 2\lambda M - q^2)}. \tag{52}$$

From the first equality in (52) for $q = 0$ we get (40) and from the second for $a = 0$ we get (40).

Assuming that $\lambda(M) < CM^\gamma$, $\gamma > 1$, from (51) we get that $a^2 + q^2 = \mathcal{O}(M^2)$. The requirement that $T \rightarrow 0$ for $M \rightarrow 0$ forces us to assume $\gamma > 2$.

Solving Equation (52) in respect to λ we get

$$\lambda_{\pm} = \frac{\pm\sqrt{-16\pi^2 a^2 T^2 - 8\pi MT + 1} - 4\pi MT + 1}{4\pi T} \tag{53}$$

Note, that q does not enter to (53). This Equation (53) is analogous to Equation (20), which does not contain Q . Equation (20) follows from (53) for $a = 0$. The equivalent representation is

$$\lambda(M) = \frac{2\pi T(2M^2 - q^2)}{1 - 4\pi MT}, \tag{54}$$

from which we get (44) for $q = 0$.

Assuming that

$$T = \sqrt{M(M_0 - M)} \tag{55}$$

and substituting this expression in (53), we get

$$\lambda_{\pm} = \lambda_{\pm}(M, M_0, a). \tag{56}$$

λ_{\pm} have different asymptotic for small M

$$\lambda_+ = \frac{1}{2\pi\sqrt{M_0 M}} + \mathcal{O}(M^{1/2}), \tag{57}$$

$$\lambda_- = 2\pi a^2 \sqrt{M_0 M} + \mathcal{O}(M^{3/2}), \tag{58}$$

and we take the second branch λ_- . On this branch we find the form of the KN black hole entropy and the free energy

$$S_{KN,-} = \pi(M + \lambda_-)^2 \tag{59}$$

$$G_{KN,-} = M - \frac{\lambda_-(M + \lambda_-)^2}{2((\lambda_- + M)^2 + a^2)} \tag{60}$$

The dependence of the entropy of radiation of KN black hole on M for the constraint corresponding to λ_- , is presented in Figure 8A. The dependence of the KN black hole entropy on M for the constraint corresponding to λ_- , is presented in Figure 8B. Here these dependences are shown by gray lines for $a = 0$ and blue lines for $a = 0.2$. In Figure 8B we show also the free energy as functions of M for zero a (brown lines for free energy) and

$a = 0.2$ (green lines for free energy) for two choices of M_0 in Equation (55), $M_0 = 0.25, 0.3$. To different choices of M_0 correspond the lines of different thickness.

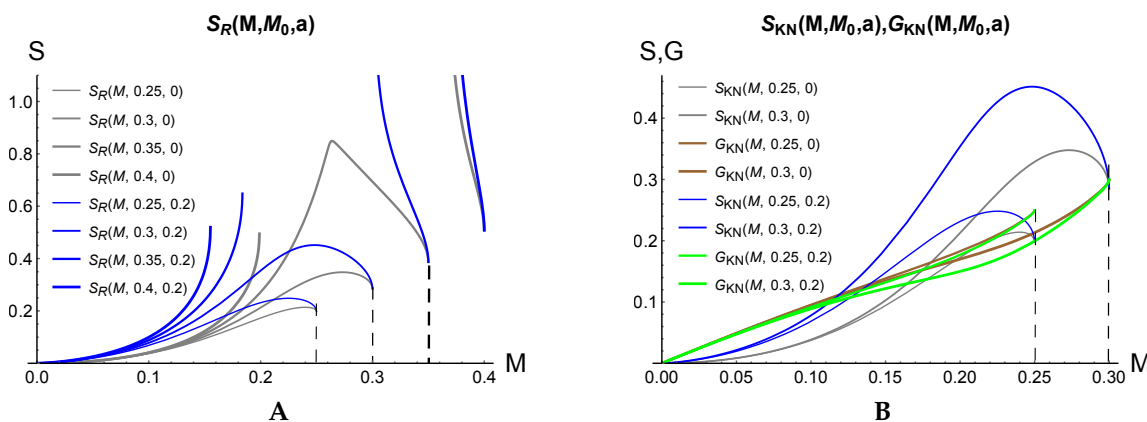


Figure 8. (A) The KN black hole entropy as function of M for special constraint providing the semi-circle dependence of temperature on M for zero a (gray lines) and $a = 0.2$ (blue lines). (B) The KN black hole entropy and free energy as functions of M for zero a (gray lines for entropy and brown lines for free energy) and $a = 0.2$ (blue lines lines for the entropy and green lines for the free energy) for two choices of M_0 in Equation (55), $M_0 = 0.25, 0.3$. To different choices of M_0 correspond the lines of different thickness.

5. Complete Evaporation of the Schwarzschild–de Sitter Black Hole

The line element has the form

$$ds^2 = -f(r)dt^2 + f(r)^{-1}dr^2 + r^2d\Omega^2, \tag{61}$$

where

$$f(r) = 1 - \frac{2M}{r} - \frac{\Lambda}{3}r^2, \tag{62}$$

M is the mass of the black-hole and $\Lambda > 0$ is the positive cosmological constant. For

$$0 < 3M\sqrt{\Lambda} < 1 \tag{63}$$

there are three horizons: the black hole horizon

$$r_+ = \frac{2}{\sqrt{\Lambda}} \sin\left(\frac{1}{3} \arcsin 3M\sqrt{\Lambda}\right), \tag{64}$$

the cosmological horizon

$$r_c = \frac{2}{\sqrt{\Lambda}} \sin\left(\frac{1}{6}\left(2 \arccos(3\sqrt{\Lambda}M) + \pi\right)\right) \tag{65}$$

and the negative non-physical one.

The Hawking temperature of Schwarzschild–de Sitter is

$$T_{SdS} = \frac{1}{4\pi r_+} (1 - \Lambda r_+^2), \tag{66}$$

where r_+ is given by (64). We can represent the temperature as

$$T_{SdS}(M, \Lambda) = \frac{1 - 4 \sin^2\left(\frac{1}{3} \arcsin(3\sqrt{\Lambda}M)\right)}{8\pi \sin\left(\frac{1}{3} \arcsin(3\sqrt{\Lambda}M)\right)} \sqrt{\Lambda} \tag{67}$$

We see that for fixed Λ the temperature becomes infinite when $M \rightarrow 0$. We note that the nominator is equal to zero at $\Lambda = 1/9M^2$ and this value of Λ realizes the bounded value of Λ admissible by inequality (63).

By analogy with the cases of RN and Kerr considered in the previous sections, we can consider Λ to be dependent on M and parametrize this dependence by a function $\lambda = \lambda(M) > 0$, i.e.,

$$\Lambda = \frac{1 - \lambda(M)^2}{9M^2}. \tag{68}$$

We assume that $\lambda = \lambda(M)$ satisfies the bounds $0 < \lambda \leq 1$. One can check that if

$$\lambda(M) = o(M), \quad M \rightarrow 0, \tag{69}$$

then $T \rightarrow 0$ as $M \rightarrow 0$.

Indeed, since now the temperature is

$$T_{SdS} = \frac{\sqrt{1 - \lambda^2}}{3M} \frac{1 - 4 \sin^2\left(\frac{\pi}{6} - \frac{1}{3} \arcsin \lambda\right)}{8\pi \sin\left(\frac{\pi}{6} - \frac{1}{3} \arcsin \lambda\right)} \tag{70}$$

and assuming (69) we get the asymptotic expansion for small M as

$$T_{SdS} = \frac{\lambda}{6\sqrt{3}\pi M} + \frac{\lambda^2}{27\pi M} + O(\lambda^3). \tag{71}$$

We see that if $\lambda \sim M^\gamma, \gamma > 1$, then $T \rightarrow 0$ when $M \rightarrow 0$.

In Figure 9 we present dependence of the temperature (red lines), the black hole entropy (blue lines), the free energy G (green) and the radiation entropy S (cyan) on M for different forms of $\lambda(M), \lambda(M) = kM^\gamma$. Here $\gamma = 0.7, 1, 1.1$ and 1.5 . Plots in darker tones correspond to $\gamma \leq 1$ and light tones to $\gamma > 1$. We see that for the later cases $T \rightarrow 0$ at $M \rightarrow 0$. To guarantee $\Lambda > 0$ it is assumed that $\lambda(M) < 1$.

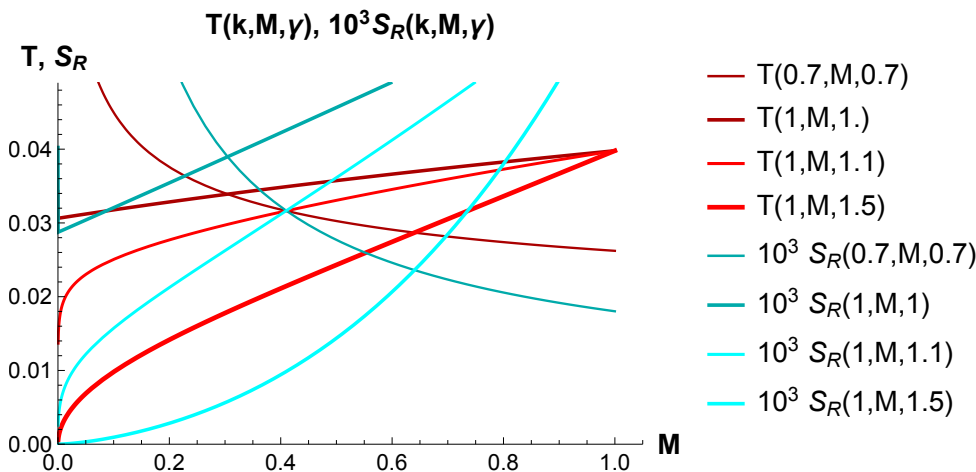


Figure 9. Cont.

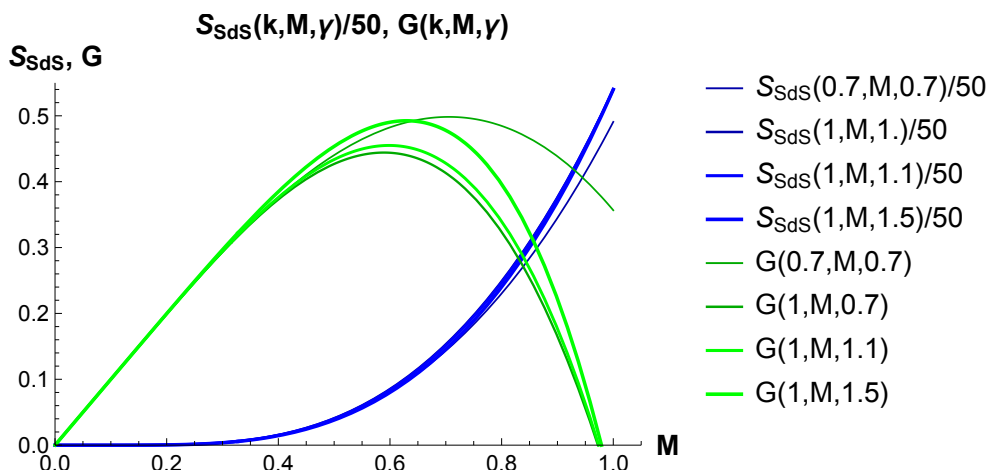


Figure 9. The plot shows the dependence of the temperature T (red), the entropy S_{SdS} (blue), the free energy G (green) and the radiation entropy S (cyan) on M for functions $\lambda(M) = kM^\gamma$ with different scaling parameter k and γ . Plots in light tones correspond to parameters describing dependencies with $T \rightarrow 0$ at $M \rightarrow 0$. Darker tones correspond to increasing temperature at $M \rightarrow 0$, or $T(0) \neq 0$ (thick darker red line, $\gamma = 1$).

6. Complete Evaporation of RNdS/AdS Black Holes

The blackening functions for the Reissner–Nordstrom–de Sitter / Anti de Sitter (RNdS / AdS) black holes are

$$f = 1 - \frac{2M}{r} + \frac{q^2}{r^2} + \epsilon \frac{r^2}{\ell^2}, \quad \frac{1}{3}\Lambda = \frac{1}{\ell^2}, \tag{72}$$

where $\epsilon = +1$ for AdS and $\epsilon = -1$ for dS.

For the dS case there is the domain of parameters ($0 \leq q \leq M \leq M_{cr}(q, \ell)$), where the equation $f(x) = 0$ has four real roots $r_{--} \leq r_- \leq r_+ \leq r_c$ where the last three roots (r_- horizon, event horizon r_+ and cosmological horizon r_c) are positive and the first r_{--} is negative. For the AdS case there is also the domain of parameters where two roots (event horizon r_+ and cosmological horizon r_c , we keep for them the same notations) are positive. The last two roots are complex. In both cases, dS and AdS, in the domain of existence of the event horizon, we obtain the expressions for the black hole mass and the temperature in term of $x \equiv r_+$ (see for example [21])

$$M = \frac{1}{2}x + \frac{q^2}{2x} + \epsilon \frac{x^3}{2\ell^2}, \tag{73}$$

$$T = \frac{1}{4\pi} \left(\frac{1}{x} - \frac{q^2}{x^3} + \epsilon \frac{3x}{\ell^2} \right). \tag{74}$$

We consider the following curve on the equation of state surface

$$q^2 = x^2 - \mu^2(x), \tag{75}$$

where the function $\lambda(x)$ satisfies the bounds

$$0 < \mu(x) \leq x. \tag{76}$$

Equation (75) gives the following expressions for M and T in terms of λ

$$M = x - \frac{\mu^2}{2x} + \varepsilon \frac{x^3}{2\ell^2}, \tag{77}$$

$$T = \frac{1}{4\pi x} \left(\frac{\mu^2}{x^2} + \varepsilon \frac{3x^2}{\ell^2} \right). \tag{78}$$

We denote by $m(x)$ the expression

$$m(x) = x - \frac{\mu^2}{2x} + \varepsilon \frac{x^3}{2\ell^2} \tag{79}$$

The function $\lambda(x)$ should be such that Equation (77)

$$M = m(x), \tag{80}$$

has a positive solution $x = x(M)$ for sufficiently small M . We suppose that $m'(x) > 0$ for small $x \geq 0$, $m(0) = 0$, then $m(x)$ is an increasing function and Equation (80) has a unique positive solution for sufficiently small M . Hence the function $\lambda(x)$ should satisfy the following relation for small x

$$\left(\frac{\mu(x)^2}{2x} \right)' < 1 + 3\varepsilon \frac{x^2}{2\ell^2} \tag{81}$$

Furthermore, to obtain M and T vanishing in the limit $x \rightarrow 0$ we assume the bound

$$\mu(x) = o(x^{3/2}) \tag{82}$$

In the next subsections we demonstrate numerically behaviour of temperature along the curves (75)

6.1. RNdS

Let us first consider the RNdS case, $\varepsilon = -1$, in more detail. For instance, we can take

$$\mu(x) = Cx^\alpha. \tag{83}$$

- All the requirements (including the positivity of the temperature) are satisfied if

$$\frac{3}{2} < \alpha < 2, \tag{84}$$

see Figure 10. In the top of Figure 10A we present the dependence of temperature on mass M and q (the cyan surface). The coloured curves show dependencies of temperature along curves $q = q(x)$ given by Equations (75) and (83) with different γ under restriction (84) and $C = 1$, here $\ell = 1$. In the right plot we also show this dependence at $\ell = \infty$ (the pink surface). In both cases the curves are very closed to the critical line $M = q$.

- $\gamma = 2$ corresponds to

$$q = x\sqrt{1 - Cx^2} \tag{85}$$

The behaviour of temperature along the curves (85) for $x \rightarrow 0$ is presented on Figure 11. As in Figure 10 cyan and pink surfaces show the dependence of temperature on mass M and q for $\ell = 1$ and $\ell = \infty$, respectively. The coloured curves show dependence of the temperature along curves (85) for different C . As in the previous case the curves are very closed to the critical line $M = q$.

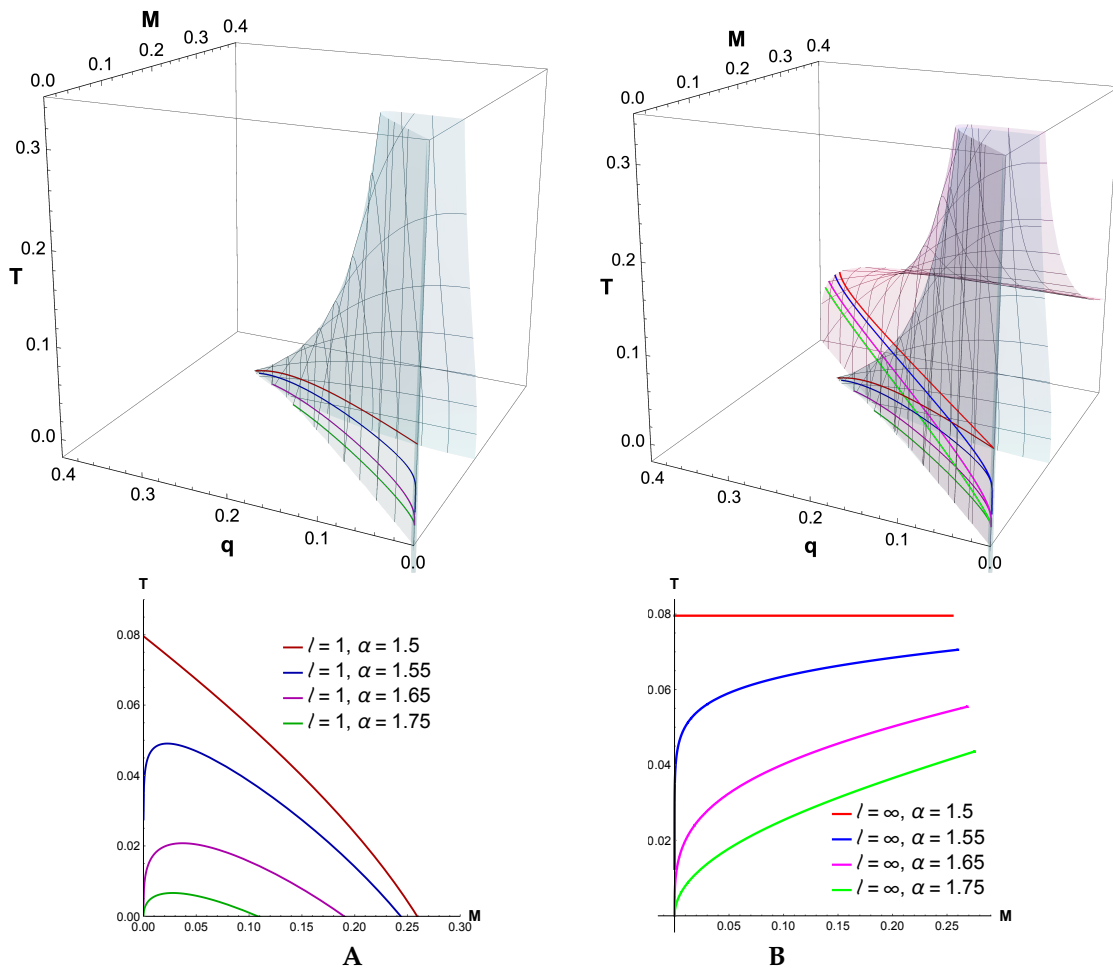


Figure 10. (A). Top: The cyan surface shows the dependence of temperature on mass M and q . The coloured curves show dependencies of temperature along curves $q = q(x)$ given by Equations (75) and (83) with different γ . Here $\ell = 1$. Bottom: dependence of the temperature along the curves given by Equations (75) and (83) with different γ indicated on the legends to this plot. (B). Top: The pink surface show the dependence of temperature on mass M and q for flat case ($\ell = \infty$). The light coloured curves show dependencies of temperature along curves $q = q(x)$ given by Equations (75) and (83) with different γ for flat case. The cyan surface and darker curves are the same as on (A).

From Figure 10 we see that all curves with $\alpha > \alpha_{cr} = 1.5$ that show vanishing of the temperature for $M \rightarrow 0$. This concerns the finite ℓ , Figure 10A, as well as $\ell \rightarrow \infty$, Figure 10B. Note that vanishing of the temperature at $M \rightarrow 0$ show all curves with $\gamma > \gamma_{cr} = 2$ presented in Figure 2A. Let us explain relation between these critical $\alpha_{cr} = 1.5$ and $\gamma_{cr} = 2$. To this purpose let compare the parametrization used near $M \rightarrow 0$ in Section 2 and parametrization near $M \rightarrow 0$ used here,

$$q^2 = M^2 - \lambda^2(M) \tag{86}$$

$$q^2 = x_+^2 - \mu^2(x_+) \tag{87}$$

Taking into account relation (77) at $\ell = \infty$, i.e.,

$$M = x_+ - \frac{\mu^2}{2x_+}, \tag{88}$$

and (86) and (86) we get

$$\mu^2(x_+) = x_+^2 - (x_+ - \frac{\mu^2}{2x_+})^2 + \lambda^2(x_+ - \frac{\mu^2}{2x_+}) \tag{89}$$

Supposing that

$$\mu(x) = x^\alpha, \quad \lambda(M) = \left(\frac{M}{m_0}\right)^\gamma \tag{90}$$

we get equation

$$F(x, \alpha, \gamma) = \left(\frac{x}{m_0}\right)^{2\gamma} \left(1 - \frac{1}{2}x^{2(\alpha-1)}\right)^{2\gamma} - \frac{1}{4}x^{4\alpha-2} \tag{91}$$

If $\alpha > 0$ for small x in the leading order we get identity if

$$m_0^\gamma = 2, \quad \gamma = 2\alpha - 1. \tag{92}$$

In particular, we see that $\alpha = 3/2$ correspond to $\gamma = 2$. This is in agreement with plots presented in Figures 2A and 10B, since in both case the temperature go to constant values for $\alpha = 3/2$ and $\gamma = 2$, respectively.

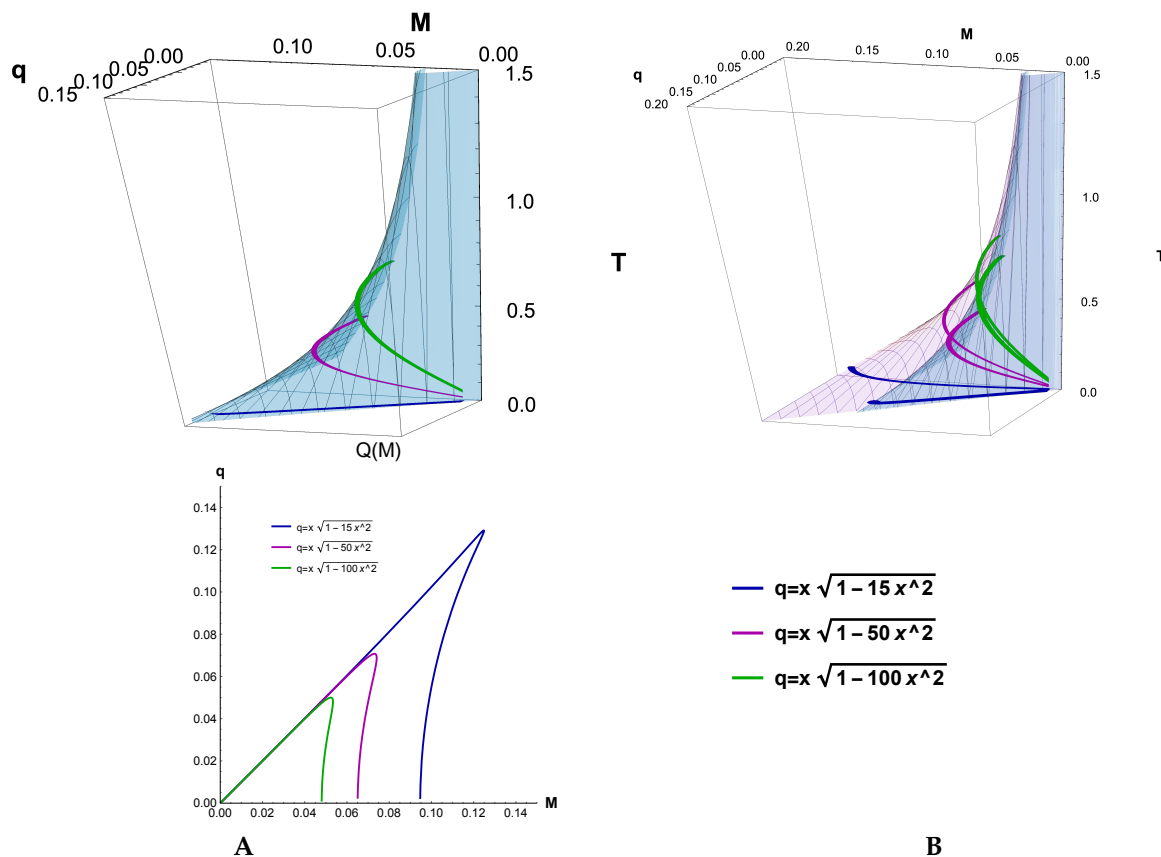


Figure 11. The cyan surface in the top of the coulomb (A) shows the temperature dependence of the black hole temperature on the black hole mass M and the charge q for $\ell = 0.5$. The coloured curves show dependence of the temperature along spacial curves $q = x\sqrt{1 - Cx^2}$. A top view on the curves depicted in the 3D plot shown in the top line of (A) is shown in the bottom of (A). The pink surface in the top of the coulomb (B) shows the temperature dependence of the black hole temperature on the black hole mass M and the charge q for $\ell = \infty$. The cyan surface here is the same as in (A). The coloured curves here correspond to $q = x\sqrt{1 - Cx^2}$ on both surfaces.

One can use another parametrization of mass, charge and cosmological constant and obtain results similar to results obtained above. In this parametrization mass and

cosmological constant are written in terms of ratio of event horizons to cosmological horizon, $x = r_+/r_c$ and the electric charge q [22]

$$M = \frac{(x + 1)(x^2 r_c^2 + q^2 x^2 + q^2)}{2x(x^2 + x + 1)r_c}, \quad x = r_+/r_c \tag{93}$$

$$\Lambda = \frac{3(xr_c^2 - q^2)}{x(x^2 + x + 1)r_c^4} \tag{94}$$

The expressions for temperatures for black hole horizon reads

$$T_+ = \frac{(x - 1)(q^2(x(3x + 2) + 1) - r_c^2 x^2(2x + 1))}{4\pi x^3(x^2 + x + 1)r_c^3} \tag{95}$$

$$T_c = \frac{(x - 1)(x(x + 2)r_c^2 - q^2(x(x + 2) + 3))}{4\pi x(x^2 + x + 1)r_c^3} \tag{96}$$

We set

$$q^2 = x^2 r_c^2 - \rho^2(x) \tag{97}$$

One can see that if $\rho(x)$ satisfies for small x the bound

$$C_1 x^{\beta+3} r_c^2 < \rho^2(x) < C_2 r_c^2 x^{\beta+2}, \quad 4 > \beta > 3 \tag{98}$$

then mass (93) behaves as $M = r_c x + o(x)$ and temperatures (95) and (96) for $x \rightarrow 0$ behave as $T_+ \rightarrow 0$ and $T_c \rightarrow const.$

For example one can take in (97)

$$\rho = C_1 r_c^2 x^{\beta+3}, \tag{99}$$

then for small x we get

$$M = r_+ - \frac{1}{2} C_1 \frac{r_+^{\beta+1}}{r_c^{\beta+1}} + \dots \tag{100}$$

$$T_+ = -\frac{3r_+}{4\pi r_c^2} + \frac{C_1}{4\pi r_c^{1+\beta}} r_+^\beta + \dots, \tag{101}$$

i.e., we get that the temperature goes to zero for $\beta > 0$.

6.2. RNAdS

In this subsection we consider the AdS, and deal with Formulas (73) and (74) for mass and temperature for $\varepsilon = 1$. As in the previous subsection we consider the same parametrisation as in (75) and take

$$\lambda(x) = Cx^\gamma, \quad \frac{3}{2} < \gamma < 2 \tag{102}$$

(we take for simplicity $C = 1$) and consider the behaviour of the temperature near $x = 0$. The typical behaviour is shown in Figure 12. We see that for $\frac{3}{2} < \gamma < 2$ the temperature decreases, for $\gamma = 1.5$ goes to finite values and for $\gamma < 3/2$ goes to infinity.

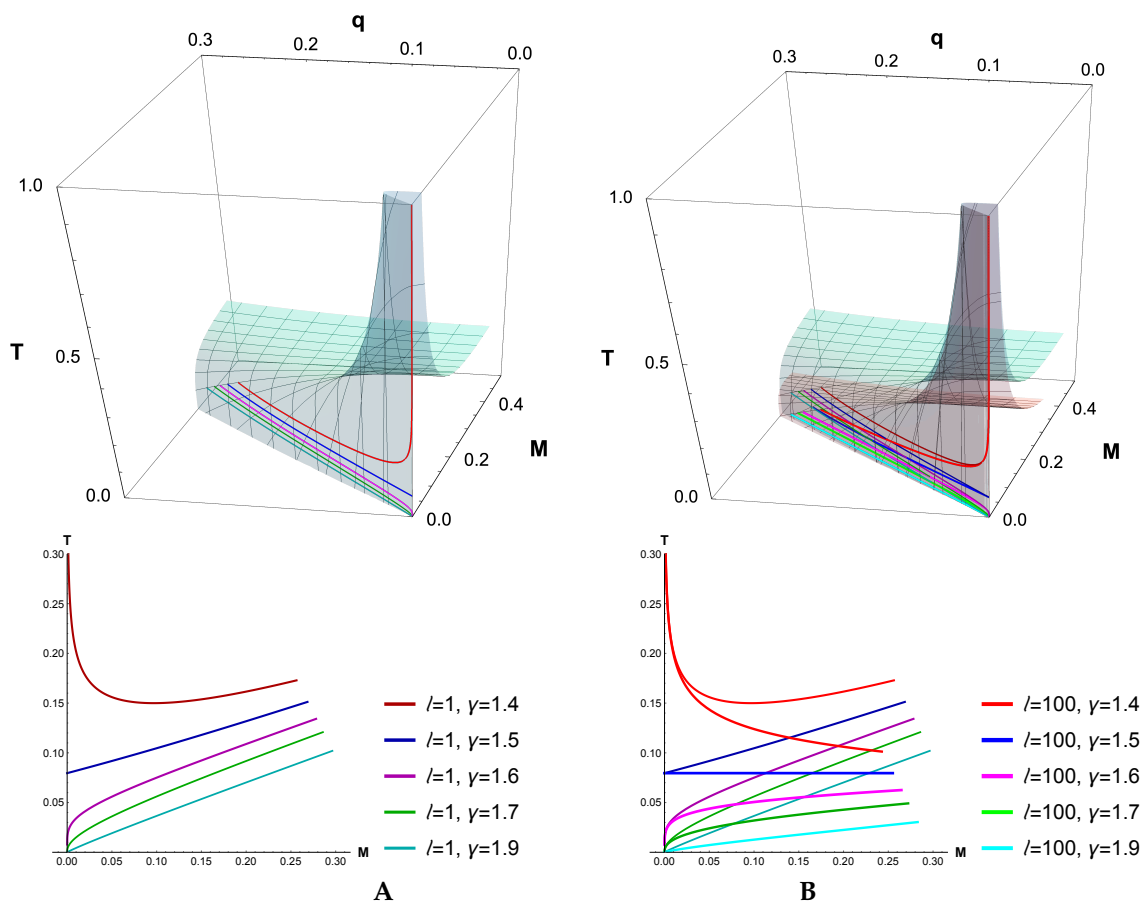


Figure 12. (A). Top: The cyan surface shows the dependence of temperature on mass M and q . The coloured curves show dependencies of temperature along curves $q = q(x)$ given by Equations (75) and (102) with different γ . Here $\ell = 1$. Bottom: dependence of the temperature along the curves given by Equations (75) and (102) with different γ indicated on the legends to this plot. (B). Top: The pink surface show the dependence of temperature on mass M and q for large ℓ ($\ell = 100$). The light-coloured curves show dependencies of temperature along curves $q = q(x)$ given by Equations (75) and (102) with different γ for large ℓ . The cyan surface and darker curves are the same as in (A).

7. Conclusions and Discussion

As already mentioned in the Introduction, the problem of complete evaporation of Schwarzschild black holes is that when the black hole mass M tends to zero, an explosion of temperature $T = 1/8\pi M$ occurs. Models of complete evaporation of black holes without blow-up of temperature are considered. In these models, the black holes metric depends not only on the mass M but also on additional parameters (thermodynamics variables) such as the charge Q and the angular momentum a and special relations between the mass and these parameters are assumed.

The Hawking temperature defines a state equation surface Σ in the space of thermodynamics variables. Curves on the surface Σ such that evaporation along them provides complete evaporation without blow-up of temperature are described. In the models under consideration, there are two possible forms of projections of these curves on (M, Q) -plane (here Q can be Q or a), see Table 1.

- In the first case, we are dealing with a deformed bell form of constraint (see a schematic plot in the first row, first coulomb in Table 1). Under additional restrictions on the parameter γ , specifying the form of constraints (3) with (22), ($\gamma > 2$ in the text), we get complete evaporation of black holes with zero temperature at the end of evaporation. The Hawking temperature and the radiation entropy for this case first increase with decreasing of mass and get the maximal values, then they begin to decrease to zero

values at zero mass (see a schematic plot in the first row, second and third coulombs in Table 1). Increasing of temperature with decreasing of mass corresponds to increasing of radiation entropy. Comparing the plot in the first row, first coulomb, Table 1 and the plot in the first row, second coulomb, Table 2, we see that recharging of the black hole is accompanied by increasing of free energy, that requires some extra forces.

- In the second case, constraints are given by curves in the (M, Q) -plane that correspond to small deviations from corresponding extremal curves (see a schematic plot in the second row, first coulombs in Table 1). The mass dependence of temperature has the form of the semi-circle and the dependence of the radiation entropy on mass has the bell-shaped form (plots in the second row, second and third coulombs in Table 1). The plots in second row of Table 2 show dependencies $S_{BH}(M)$, $G(M)$ and $S_R(T)$.

Table 1. Evaporation curves in (M, Q) , (M, T) and (M, S_R) -planes.

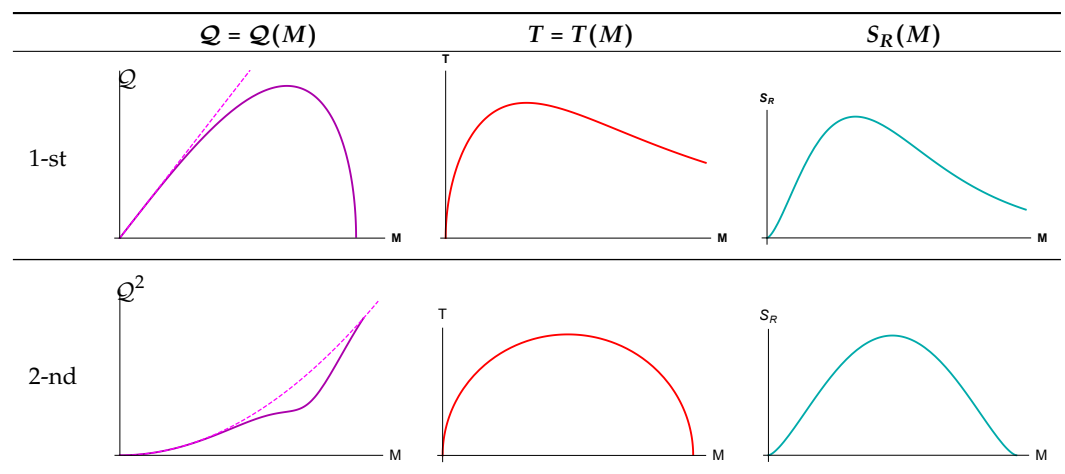
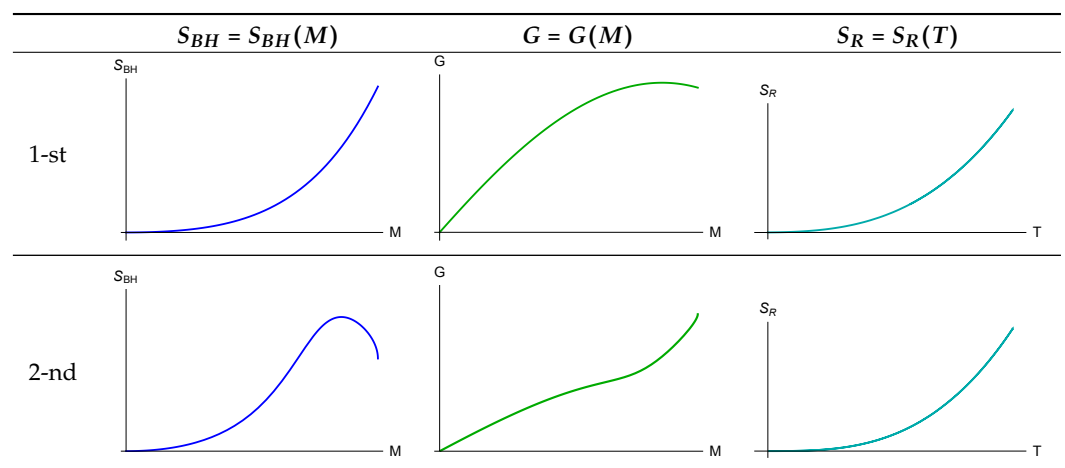


Table 2. Evaporation curves in (M, S_{BH}) , (M, G) and (T, S_R) -planes.



Summing up the consideration in asymptotically flat cases we obtain the mass dependence of the entropy of radiation, which is schematically presented in Figure 5B, or in the third column of Table 1. Assuming a slow monotonic dependence of the mass on the time during the evaporation of the black hole, from such mass dependence of the radiation entropy we get the Page curve for time dependence of the radiation entropy. We also generalised the above consideration to the case of Schwarzschild–de Sitter and Reissner–Nordstrom-(Anti)-de Sitter black holes.

An important question is why the black holes follow evaporation curves avoided the blow-up of temperature? If one means realistic black holes, this question could be answered

in the spirit of the anthropic principle, since otherwise an explosion of temperature occurs. Or in other words, we can say that we have to use a kind of black hole censorship.

The problem of complete evaporation is also discussed in [23], where the singularity of temperature is attributed to the singularity of the Kruskal coordinates in the limit $M \rightarrow 0$ and alternative coordinates are proposed which describe a temperature distribution and are regular for vanishing mass.

Author Contributions: Conceptualization, methodology, investigation, I.A. and I.V.; writing original draft preparation, I.V.; writing, review and editing, I.A. All authors have read and agreed to the published version of the manuscript.

Funding: This work was supported by the Russian Science Foundation (Project 19-11-00320, Steklov Mathematical Institute).

Data Availability Statement: Not applicable

Acknowledgments: We would like to thank Victor Berezhin, Valery Frolov and Michael Khramtsov for useful discussions and remarks.

Conflicts of Interest: The authors declare no conflict of interest.

References

1. Hawking, S.W. Particle creation by black holes. *Comm. Math. Phys.* **1975**, *43*, 199. [[CrossRef](#)]
2. Hawking, S.W. Breakdown of Predictability in Gravitational Collapse. *Phys. Rev. D* **1976**, *14*, 2460–2473. [[CrossRef](#)]
3. Page, D.N. Time Dependence of Hawking Radiation Entropy. *JCAP* **2013**, *2013*, 28. [[CrossRef](#)]
4. Susskind, L.; Lindesay, J. *Introduction To Black Holes, Information And The String Theory Revolution, An: The Holographic Universe*; World Scientific: Singapore, 2004.
5. Frolov, V.; Novikov, I. *Black Hole Physics: Basic Concepts and New Developments*; Springer Science, Business Media: Berlin/Heidelberg, Germany, 2012; Volume 96.
6. Hawking, S.W. Black hole explosions? *Nature* **1974**, *248*, 30–31. [[CrossRef](#)]
7. Page, D.N. Information in Black Hole Radiation. *Phys. Rev. Lett.* **1993**, *71*, 3743. [[CrossRef](#)]
8. Penington, G. Entanglement Wedge Reconstruction and the Information Paradox. *JHEP* **2020**, *9*, 2. [[CrossRef](#)]
9. Almheiri, A.; Engelhardt, N.; Marolf, D.; Maxfield, H. The entropy of bulk quantum fields and the entanglement wedge of an evaporating black hole. *JHEP* **2019**, *12*, 63. [[CrossRef](#)]
10. Almheiri, A.; Mahajan, R.; Maldacena, J.; Zhao, Y. The Page curve of Hawking radiation from semiclassical geometry. *JHEP* **2020**, *3*, 149. [[CrossRef](#)]
11. Aref'eva, I.; Rusalev, T.; Volovich, I. Entanglement entropy of near-extremal black hole. *Theoret. Math. Phys.* **2022**, *212*, 1284–1302. [[CrossRef](#)]
12. Gibbons, G.W. Vacuum polarization and the spontaneous loss of charge by black holes. *Commun. Math. Phys.* **1975**, *44*, 245. [[CrossRef](#)]
13. Zaumen, W.T. Upper bound on the electric charge of a black hole. *Nature* **1974**, *247*, 530–531. [[CrossRef](#)]
14. Carter, B. Charge and particle conservation in black-hole decay. *Phys. Rev. Lett.* **1974**, *33*, 558. [[CrossRef](#)]
15. Damour, T.; Ruffini, R. Quantum electro-dynamical effects in Kerr-Newmann geometries. *Phys. Rev. Lett.* **1975**, *35*, 463. [[CrossRef](#)]
16. Page, D. Particle emission rates from a black hole. II. Massless particles from a rotating hole. *Phys. Rev. D* **1976**, *14*, 3260. [[CrossRef](#)]
17. Hiscock, W.A.; Weems, L.D. Evolution of charged evaporating black holes. *Phys. Rev. D* **1990**, *41*, 1142. [[CrossRef](#)] [[PubMed](#)]
18. Gabriel, C. Spontaneous loss of charge of the Reissner-Nordström black hole. *Phys. Rev. D* **2000**, *63*, 24010. [[CrossRef](#)]
19. Sorkin, E.; Piran, T. Formation and evaporation of charged black holes. *Phys. Rev. D* **2001**, *63*, 124024. [[CrossRef](#)]
20. Ong, Y.C. The attractor of evaporating Reissner–Nordström black holes. *Eur. Phys. J. Plus* **2021**, *136*, 61. [[CrossRef](#)]
21. Li, H.F.; Ma, M.S.; Ma, Y.Q. Thermodynamic properties of black holes in de Sitter space. *Mod. Phys. Lett. A* **2016**, *32*, 1750017. [[CrossRef](#)]
22. Zhang, Y.; Ma, Y.b.; Du, Y.Z.; Li, H.F.; Zhang, L.C. Phase transition and entropy force in Reissner-Nordström-de Sitter spacetime. *arXiv* **2022**, arXiv:2204.05621.
23. Aref'eva, I.; Volovich, I. Quantum explosions of black holes and thermal coordinates. *Symmetry* **2022**, *14*, 2298. [[CrossRef](#)]

Disclaimer/Publisher's Note: The statements, opinions and data contained in all publications are solely those of the individual author(s) and contributor(s) and not of MDPI and/or the editor(s). MDPI and/or the editor(s) disclaim responsibility for any injury to people or property resulting from any ideas, methods, instructions or products referred to in the content.